

## 2 Photosystem I

### 2.1 Structure of PS I [1].

Photosystem I is the complex in the thylakoid membrane that mediates the light induced transfer of electrons from plastocyanin, a mobile electron carrier located in the lumen, to ferredoxin on the stromal membrane side. PS I is a large multi-subunit protein complex, comprised of 12 individual polypeptides [2]. The whole complex consists of an integrated light-harvesting complex (antenna system) and a core electron transfer chain. The light harvesting complex serves as an antenna to trap light and funnel its energy to the reaction center core complex. PS I contains about 96 chlorophylls, 22 carotenoids, 3 [Fe<sub>4</sub>S<sub>4</sub>] clusters and 2 phylloquinones [3].

In 2001, the X-ray structure of PS I was solved at 2.5Å resolution [1, 4]. This provides unique structural information. Isolated cyanobacterial PS I exists as a trimer (relative molecular mass:  $M_r = 3 \times 356,000$ ). The trimer has a threefold rotation axis ( $C_3$ ), which is perpendicular to the membrane plane. The PsaL protein located in the 'trimerization domain' forms most of the contacts between the monomers. The large ( $M_r = 83K$ ) subunits PsaA and PsaB are related by pseudo- $C_2$  axis located at the center of the PS I monomer and oriented parallel to the  $C_3$  axis. The organic cofactors of the electron transfer chain (ETC) are arranged in two branches along the pseudo- $C_2$  axis, and most of the antenna chlorophyll (Chl *a*) molecules, the carotenoids and the lipids are bound to PsaA/B. The electron transfer chain of PS I is formed by six chlorophylls, two phylloquinones and three Fe<sub>4</sub>S<sub>4</sub> clusters (Figure 2.1). The cofactors forming one branch are not bound exclusively to one subunit of PS I, the crossovers being eC-B2 and eC-A2 accessory chlorophylls molecules.

Charge separation is initiated at the primary electron donor  $P_{700}$ , heterodimer formed by Chl  $a$ /Chl  $a'$  chlorophyll molecules (eC-A1/eC-B1). The chlorin planes of these chlorophylls are parallel at 3.6 Å interplanar distance and oriented perpendicular to the membrane plane.

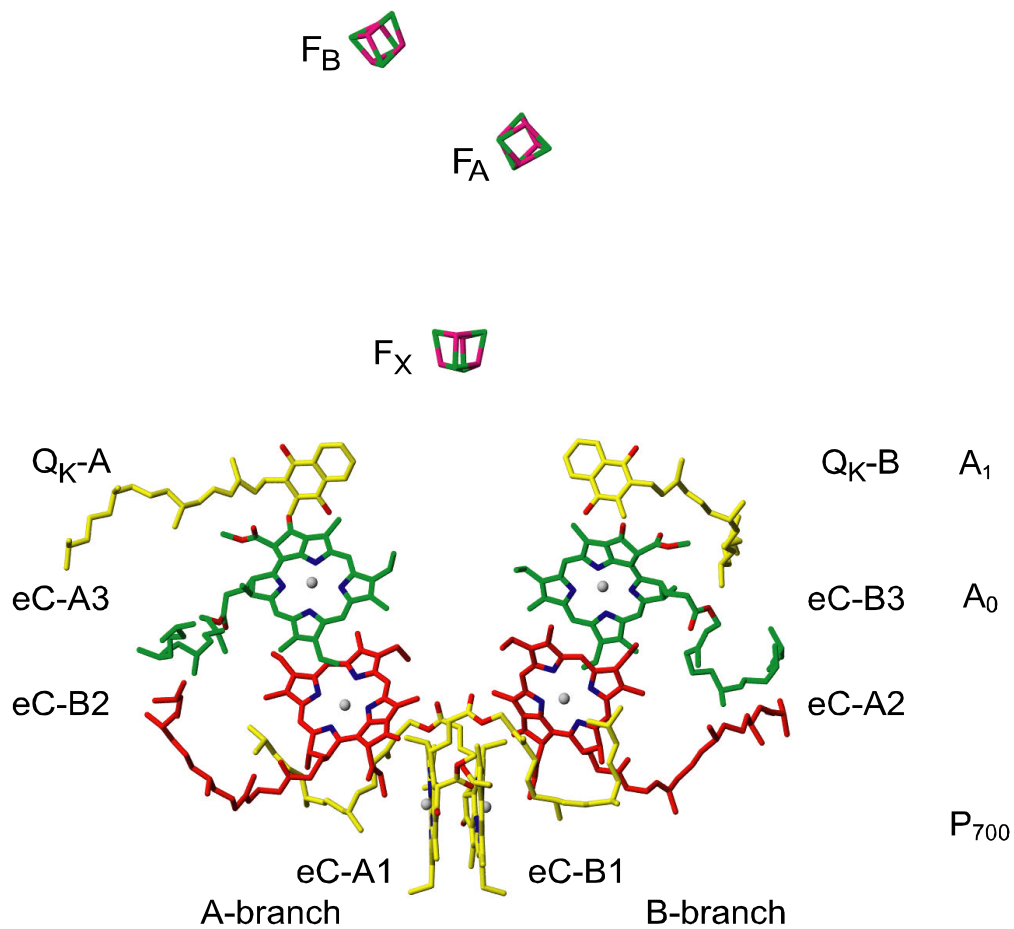


**Figure 2.1** Cofactors of the electron transfer chain in PS I. Note the  $C_2$ -symmetric arrangements of cofactors in A and B-branches. The symmetry axis is parallel to membrane normal and is passing through  $F_X$  [1] (pdb entry **1JB0**).

A  $Mg^{2+}$  ion is co-ordinated with each of chlorophylls: the  $Mg^{2+}$  ion coordinated with the eC-A1 chlorophyll has an additional ligand, the histidine A-680His, the other  $Mg^{2+}$  ion is coordinated with the eC-B1 chlorophyll and B-660His. The distance between the  $Mg^{2+}$  ions is 6.3Å. In contrast to the homodimeric special pair in the bacterial reaction center (bRC),  $P_{700}$  is a heterodimer, eC-B1 being Chl *a* and eC-A1 being Chl *a'*, the C13<sup>2</sup> epimer of Chl *a*. The asymmetry extends to the binding pockets for the two chlorophylls. The side chains of the transmembrane  $\alpha$ -helices A-i and A-k and a water molecule form hydrogen bonds to Chl *a'* eC-A1, whereas no hydrogen bonds are found to Chl *a* eC-B1. The chlorophylls of the second pair of Chl *a* molecules next to  $P_{700}$ , eC-A2/eC-B2, are not engaged in any hydrogen bonds. Their  $Mg^{2+}$  ions are coordinated by water molecules hydrogen-bonded to side chain of Asn A604 and Asn B591, respectively. The eC-A3/eC-B3 Chl *a* molecules are coordinated by sulphur atoms of Met A668 and Met B668 (distance  $Mg^{2+} - S = 2.6\text{\AA}$ ). Short hydrogen bonds are donated by the hydroxyl groups of tyrosines A696 and B676 to the respective keto oxygens of ring V of eC-A3 and eC-B3. All the amino acids involved in  $Mg^{2+}$  coordination and hydrogen bonding to the second and third Chl *a* pairs of the ETC are strictly conserved between PsaA and PsaB from cyanobacteria to higher plants, suggesting that these protein-chlorophyll interactions are essential for fine-tuning the redox potentials of the cofactors [5].

The phylloquinone molecule is the secondary electron acceptors in the ETC. Quinone  $Q_k$ -A and  $Q_k$ -B planes are  $\pi$ -stacked at 3.0-3.5Å with indole rings of conserved Trp A697 and B677 on the stromal surface  $\alpha$ -helices A/B-jk. Only the carbonyl oxygen atom in ortho position to the phytyl chain accepts hydrogen bonds from backbone -NH-group of Leu A722 ( $Q_k$ -A) and Leu B706 ( $Q_k$ -B).

The [4Fe4S] cluster Fx is a cube. It is situated directly on the pseudo- $C_2$  axis running through PS I heterodimer. Fx is coordinated by fully conserved, identical

sequences on PsaA and PsaB. Each of those sequences provides two cysteine ligands to the cluster. The next electron acceptors are two 4Fe4S clusters called  $F_A$  and  $F_B$ . They are bound to the PsaC protein. The structure shows that the cluster located at a center to center distance of  $15\text{\AA}$  to  $F_X$  is  $F_A$ , and the second at a distance of  $22\text{\AA}$  to  $F_X$  is  $F_B$ .

## 2.2 Function of PS I [4].

The three-dimensional structure of cyanobacterial PS I at  $2.5\text{\AA}$  resolution provides key information about structural details required for a detailed understanding of its function on the basis of protein cofactor interactions. At the same time the function of cofactors in the electron transfer process are still under discussion. The most important is the interaction between protein and cofactors leading to the changes in their redox properties, energetic and kinetic of electron transfer in protein. For comparison, the redox potentials of the cofactors in PS II are shifted  $600\text{mV}$  high (more positive) than in PS I in order to be coupled with the water splitting process while the cofactors in PS I have more negative redox potentials in order to be able to reduce ferredoxin (or flavodoxin) [6].

The directionality of light-induced electron transfer has been a long-standing issue in the study of photosynthetic reaction centers. Electron transfer is exclusively unidirectional in Type II reaction centers such as PS II and bRC. In those protein complexes a single turnover results in the reduction of  $Q_B$  to a semiquinone and a second turnover results in the double reduction (and double protonation) of  $Q_B$  to a hydroquinone. The stability of  $Q_B^-$  requires that there is no recombination pathway; hence, there is also no direct forward pathway to  $Q_B$ . The reduced hydroquinone in the  $Q_B$  site is loosely bound and is replaced by an oxidized quinone, thereby recharging the site for a new round of light-induced turnover [7]. In PS I, a single turnover results in the reduction of the quinone

to a semiquinone; the electron is then passed to an interpolypeptide iron-sulphur cluster  $F_X$ . As a result, there is only the need for a one-electron reduction of a single quinone to the semiquinone state [8]. In PS I there is no *a priori* reason that electron transfer must be either uni- or bi-directional because there is no obvious need for one-electron  $Q_A$ -type and for a 2-electron  $Q_B$ -type quinone as in the bacterial reaction center.

### 2.2.1 $P_{700}$ primary donor

The charge separation process starts after  $P_{700}$  is excited to its lowest excited state,  $P_{700}^*$ , and an electron is very rapidly (within 1- 2 ps) transferred to  $A_0$  [9], Figure 2.2. However, this is the most probable pathway there are some alternative mechanisms available in the literature especially for the bRC and PS II which consider the additional (or preceding) excitation of accessory chlorophylls [10, 11]. The initial electron transfer steps in PS I are difficult to observe because the trapping of the excitation from the antenna, which has lifetime of about 30 ps, masks these early events. Thus, it is difficult to prove the 1- 2 ps time constant for the initial charge separation step.  $P_{700}^*$  has a highly negative redox potential (about -1300 mV), making it a very strong reductant. The reaction free energy  $\Delta G_0$  for the initial charge separation step was estimated to be 250 meV [12]. Investigation of the triplet state of  $P_{700}$  ( $^3P_{700}$ ) and the cation  $P_{700}^{+\bullet}$  by magnetic resonance and infrared spectroscopic techniques clearly shown that it has a dimeric nature [13, 14]. The spin density in  $P_{700}^{+\bullet}$  is unequally distributed between the two chlorophylls. About 85% of the spin density is located on one of the two chlorophylls in  $P_{700}^{+\bullet}$  [15]. Recent mutagenesis studies indicate that the spin carrying chlorophyll is coordinated by histidine in PsaB [16, 17, 18]. As described already in Chapter 2, section 2.1.,  $P_{700}$  primary donor represents a heterodimer and chlorophyll molecules have different numbers of hydrogen bonds with the protein. This structural information about the inequivalence of the chlorophylls in  $P_{700}$  correlates perfectly with the spectroscopic results. Differences in the

structures of the chlorophyll molecules and their interactions with the protein might be the reason for the preferential activity of one branch in the electron transfer process *versus* the other.

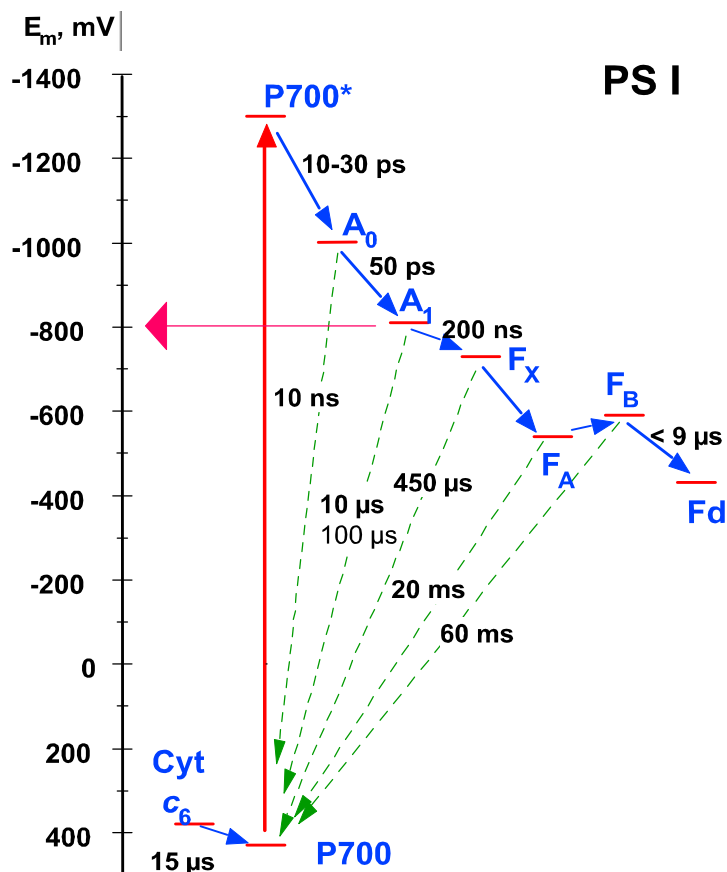


**Figure 2.2** Energetic of charge separation in Photosystem I [43]. Time constants of electron transfer and recombination at room temperature are indicated. The back reaction rates refer to conditions under which the subsequent electron acceptor has been removed, either biochemically or genetically. The back reaction pathways are depicted as direct to  $P_{700}$  for the sake of clarity; the actual pathways likely proceed, at least in part, back through the electron acceptor chain. For the more information about the charge separation see chapter 2.2

### 2.2.2 $A_0$ primary acceptor

The third pair of chlorophylls (Chl *a* eC-A3 and Chl *a* eC-B3) located in the middle of the membrane plays the role of the electron acceptor  $A_0$ . The axial ligands of the  $Mg^{2+}$  ions of each of these chlorophylls are sulphur atoms of methionine residues. The concept of hard and soft acids and bases predicts only a weak interaction between the hard acid  $Mg^{2+}$  and soft base methionine sulphur. The question whether the less negative redox potential of the electron acceptor  $A_0$  (-1050 mV) is caused by lack of a strong fifth ligand to the  $Mg^{2+}$  atom of these chlorophylls remains to be answered.

The electron transfer from  $A_0^{\bullet-}$  to  $A_1$ , a phylloquinone, occurs within 20-50 ps [19, 20] (see Figure 2.2) which is faster than the electron transfer from the pheophytin to quinone in bRC [21]. The free energy gap for this step was estimated to be the order of  $\Delta G_0 = 340$  meV. It was estimated that the reorganisation energy  $\lambda$  is of the same order of magnitude as the free energy gap, i.e.  $-\Delta G_0 \cong \lambda$ , which is the optimal condition for rapid electron transfer [22].

The rate of electron transfer from  $A_0^-$  to  $A_1$  was measured by ps-ns transient absorption spectroscopy for various quinones reconstituted in PS I [23]. The free energy changes for the reaction between  $A_0$  and  $A_1$  was estimated and  $\Delta G^0$  was verified in the range of -1.1 to 0.2 eV for different quinones. The maximum rate constant ( $k$ ) of  $4.35 \cdot 10^{10} \text{ s}^{-1}$  (23 ps) was obtained in PS I containing PhQ or its analogue menaquinone in which  $\Delta G^0$  is -0.34 eV. The electron transfer occurred with slower rates ( $t_{1/e} = 30 \text{ ps} - 60 \text{ ns}$ ) with the quinones/quinonoids that gave  $\Delta G^0$  higher or lower than that of phylloquinone. The  $\log k$  vs.  $\Delta G^0$  plot thus showed an asymmetrical bell shape with the maximum at the  $\Delta G^0$  value of PhQ. [24].

### 2.2.3 Phylloquinone secondary acceptor

The phylloquinone molecule in PS I has a significantly lower redox potential (-820 mV then phylloquinone in solution or  $Q_A$  (-130 mV) in bRC and PS II [6]. Such big changes in the redox potential have not been explained yet. The acceptor following the PhQ is the first of a series of iron-sulphur clusters. Based on EPR and optical data from ( $P_{700}$ - $F_X$ ) core particles, which showed that electron transfer to  $F_X$  occurs in the absence of  $F_A$  and  $F_B$ , it was identified as  $F_X$  [25, 26]. The rate for the electron transfer step  $P_{700}^+A_1^- \rightarrow P_{700}^+F_X^-$  obtained by TR EPR at high temperature [27] (will be describe in more detail in 5.7 and 5.8) or by time-resolved optical studies of  $A_1^-$  reoxidation [12] yielded conflicting results. The characterization of  $A_1$  by optical spectroscopy was mostly based on flash-induced absorption changes attributed to formation of the pair  $P_{700}^+A_1^-$ , i.e., the  $P_{700}^+A_1^-/P_{700}A_1$  difference spectrum. The deviations between the  $P_{700}^+A_1^-/P_{700}A_1$  spectrum and  $P_{700}^+/P_{700}$  spectrum agree qualitatively with the  $A_1^-/A_1$  in the range from 250 to 450 nm. Also, it has been shown previously that absorption changes associated with  $A_1^-$  can be observed around 480 nm, although the nature of this absorption band is not fully established (an electrochromic bandshift of a nearby carotenoid due to a negative charge on  $A_1$  has been suggested [28]).

Studies using so-called PS I- $\beta$  particles from spinach showed biphasic decay attributed to  $A_1^-$  oxidation with  $t_{1/2}$  of 25 ns and 250 ns, and relative amplitudes of 65% and 35%, respectively [29]. Both kinetic phases were attributed to electron transfer from  $A_1^-$  to  $F_X$ . Studies at faster timescales with PS I particles from *Synechococcus* sp. PCC 6803 also showed an additional kinetic phase attributed to  $A_1^-$  oxidation with a  $t_{1/2}$  of 10 ns [30]. Although the faster of the two kinetic phases cannot be resolved directly by transient EPR, the observed spin polarization is sensitive to the spin dynamics of short-lived precursor states with lifetimes as short as 500 ps. Recently, the influence of the fast kinetic phase on



the spin polarization patterns of  $P_{700}^+A_1^-$  was investigated [31], and it was shown that the amplitude of the fast phase in whole cells and PS I particles of cyanobacteria could account for at most ~20% of the total amplitude. The transient EPR spectra of PS I particles isolated from spinach and *Chlamydomonas reinhardtii* show a significant influence from the fast kinetic phase [31]. However, the ratio of the fast to slow kinetic phases is not constant between different preparations; rather, PS I particles isolated from spinach showed a diminished amplitude of the optically-detected 25 ns kinetic phase when isolated using less harsh conditions, down to 30% in a particle prepared without detergent [29], while transient EPR suggests at most a very small contribution from the fast kinetic phase in spinach chloroplasts and cyanobacterial whole cells [27, 32, 33].

In contrast, recent optical studies of whole cells of *Chlamydomonas reinhardtii* [34] showed biphasic kinetics attributed to the reoxidation of  $A_1^-$  with  $t_{1/2}$  of 18 ns and  $t_{1/2}$  of 160 ns and of nearly equal amplitude. Hence, it appears that the fast kinetic phase is a property inherent to PS I but its amplitude is species dependent and sensitive to environmental conditions such as the presence of detergent. Moreover, the sensitivity to detergent-isolation is much higher in eukaryotic PS I compared to cyanobacterial PS I. While the biphasic kinetics observed in the near-UV are now generally thought to be due to electron transfer from  $A_1^-$  to  $F_X$ , the origin of the biphasic behavior remains controversial (see [35] for review). Sétif and Brettel suggested that the redox potentials of  $A_1$  and  $F_X$  are close and that the fast kinetic phase reflects the establishment of redox equilibrium between  $A_1$  and  $F_X$  [29]. This proposal was made prior to detailed knowledge of PS I structure, and does not account for the pseudo  $C_2$  symmetry cofactor branches in PS I. Therefore it pre-supposes a unidirectional pathway of electron transfer. Joliot and Joliot [34] suggested that the biphasic kinetics could come about from two of sources: two conformational states which differ by the reoxidation rate of  $A_1^-$  or the two phylloquinones

which correspond to the two branches of the PS I heterodimer involved in electron transfer. The former presupposes unidirectional electron transfer and the latter presupposes bidirectional electron transfer. The latter idea became relevant when the model of PS I based on the 6 Å crystal structure [36] showed the presence of a 2-fold axis of symmetry similar to the pseudo 2-fold axis of symmetry in the purple bRC. Due to the  $C_2$  symmetry and the obvious similarity of the PsaA and PsaB polypeptides (about 45-50% identical throughout their length) the possibility of two parallel electron transfer pathways up to  $F_X$  were considered. However, based on the structural analogies of the core of PS I to the purple bacteria reaction center, which suggested a common evolutionary origin for all photosynthetic reaction centers, it has been generally thought that electron transport in PS I is unidirectional, as it is in the type II reaction centers [37].

#### *2.2.4 Protein induced asymmetric spin density distribution over the phylloquinone*

It has been already discussed above that the hydrogen bond formation between the cofactor and protein and its strength is critical for the fine tuning of cofactor redox potential. Because the main topic of this thesis is the study of quinone properties in PS I by EPR, it is necessary to describe what kind of information related to the question of hydrogen bond formation can be extracted from the EPR spectra.

In principle, hyperfine couplings (hfc) provide information about the electronic structure of the semiquinone radical at an atomic level because they are associated with the individual nuclear spins. A feature of particular interest which is reflected in the hfc is the molecular asymmetry introduced through the interaction of the quinone with the protein environment, in particular in the form of asymmetric hydrogen bonds to the carbonyl groups. Asymmetric alternating spin density distribution over the quinone ring as introduced by predominant H-bonding to one of the C=O groups has been studied in considerable detail for the corresponding  $Q_A$  site in purple bacterial reaction center

(pbRC), as reviewed recently [38]. The asymmetry in the spin density distribution has been confirmed experimentally by selective isotope labeling of several ring positions, in particular both carbon nuclei of the C=O groups. Simple MO models predict an alternating spin density distribution across the ring with dominant spin densities at ring carbon forming carboxyl group accepting stronger hydrogen bond and carbon connected with isoprenoid chain [38]. Therefore the hfs coupling of the first methylene protons of the tail is large and can be measured readily by ENDOR spectroscopy [39].

The data on spin density distribution over  $A_1^-$  in PS I are less complete. However, in contrast to the behaviour in bRC, the proton hfc of the methyl group increase relative to those observed in 2-propanol [40]. So far the  $\beta$ -methylene couplings could not be determined reliably. Nevertheless, the large hfc constants of the methyl protons indicate already that the spin density distribution of  $A_1^-$  in PS I is also asymmetric and that the asymmetry is opposite to that in  $Q_A^-$ . In contrast to  $A_1$  in PS I, the C=O group of  $Q_A$  in bRC with the dominant H-bond is meta to the ring position at which the tail is attached.

#### *2.2.5 Electron transfer to external electron carriers*

At the stromal (cytoplasmic) side, the electron is donated by  $F_B$  to ferredoxin (or flavodoxin) and thence transferred to  $NADP^+$  reductase. The reaction cycle is completed by re-reduction of  $P_{700}^{+\bullet}$  by cytochrome  $c_6$  (or plastocyanin) at the inner (luminal) side of the membrane. The electron carried by cytochrome  $c_6$  is provided by PS II *via* a pool of plastoquinone and the cytochrome  $b_6/f$  complex.

